Electronic Supplementary Material (ESI) for Sustainable Energy & Fuels.

Supporting Information

Alloying Ni_4Mo for Efficient Alkaline Hydrogen Oxidation and Hydrogen Evolution Reactions

Pengfei Cao, Xinxin Zhang, Lei Wang* and Honggang Fu*

Key Laboratory of Functional Inorganic Materials Chemistry, Ministry of Education of the People's Republic of China, Heilongjiang University, Harbin 150080 (China).

E-mail: wanglei0525@hlju.edu.cn, fuhg@hlju.edu.cn, fuhg@vip.sina.com.

Experimental section

1. Synthesis of Ni_4Mo/rGO

The graphene oxide (GO) was prepared by a Hummer' method. For the synthesis of Ni_4Mo/rGO, 50mg GO was uniformly dispersed into 50 mL deionized water and then stirring for 6 h. Subsequently, 0.006 mol $NiCl_2 \cdot 6H_2O$ and 0.0015mol $Na_2MoO_4 \cdot 2H_2O$ were added and continually stirring for 3 h. Then, 10 mL 0.2 M $NaBH_4$ aqueous solution was slowly added into 5 mL to the above solution and stirring for 2h. After centrifuging, washing and drying, the obtained precursor was pyrolyzed at 500 °C for 2 h with a promoting temperature speed of 5°C/min under a mixed atmosphere of H_2/Ar (volume ratio of 1:9). Finally, the Ni_4Mo/rGO sample was prepared. As compared, the Ni/rGO sample was synthesized by the same strategy without adding $Na_2MoO_4 \cdot 2H_2O$.

2. Characterizations

The morphology and structure were characterized by scanning electron microscopy (SEM: Hitachi S-4800) with an acceleration voltage of 5 kV and transmission electron microscopy (TEM: JEM-2100) with an acceleration voltage of 200 kV. X-ray diffraction (XRD) patterns were measured on a Bruke D8 diffractometer using Cu K_α (λ = 1 5406 Å) radiation with an accelerating voltage of 40 kV and an applied current of 20 mA. Raman spectra were performed on a Jobin Yvon HR 800 micro-Raman spectrometer at 457.9 nm. X-ray photoelectron (XPS) analyses was tested on a VG Escalab MKII spectrometer with a Mg K_α achromatic X-ray source. N_2 adsorption-desorption isotherms were tested by a Tristar II instrument from Micromeritics.

3. Electrochemical measurements

The HOR performance was evaluated using a typical three-electrode system on a Pine Instrument Company biopotentiostat. A Pt foil (1.0 cm^2) and a reversible hydrogen electrode (RHE) were used as the counter electrode and reference electrode, respectively. A rotating disk electrode (RDE) with a glassy carbon disk (diameter: 4 mm) was employed as the working electrode. The working electrode was prepared as follows: 5 mg of the catalyst was added to 2 mL of 0.125 wt% nafion ethanol solution and then sonicating for 1 h to ensure uniform dispersion. Afterwards, 40 μL of the

catalyst ink was dropped onto the surface of glassy carbon disk and dried by a lamp. Prior to the HOR measurements, H_2 was bubbled through the 0.1 M KOH electrolyte for 30 min. The LSV curves were collected at a scan rate of 10 $mV \cdot s^{-1}$ with a rotating of 1600 rpm.

The HER performance was tested on a CHI 760E Electrochemical Workstation. To prepare the working electrode, 5 mg catalyst was dispersed in 1 mL water/ethanol mixture (v/v=1:1). Subsequently, 20 μL of nafion solution (0.5 wt%) was added into the mixture. The solution was ultrasonically dispersed to obtain a well-distributed slurry, which was then pasted onto a treated NF current collector plate (1.0 × 1.0 cm^2). A graphite rod and an Hg/HgO electrode were adopted as the counter electrode and reference electrode, respectively. Prior to the electrochemical measurements, the 1.0 M KOH electrolyte solution was purged with N_2 gas for 1 h to remove any dissolved gas. The LSV curves were tested at a scan rate of 5 $mV \cdot s^{-1}$.

4. Assembly and test of APMFC

For the preparation of catalyst ink, Ni_4Mo/rGO as anode and commercial 20 wt% Pt/C as cathode were respectively dispersed in an isopropanol and water mixture (volume ratio 9:1) diluted with 5 wt% nafion. Then, it was ultrasonic treated and stirred to form a homogeneous catalyst ink. An ultrasonic sprayer was utilized to deposit the catalyst ink onto a nafion membrane with an effective area of 2 cm×2 cm, achieving a catalyst loading of 1.5 mg cm^{-2} for anode and 0.4 mg_{Pt} cm^{-2} cathode. Finally, the catalyst-coated membrane was sandwiched between two gas diffusion layers (SGL Carbon H24XC483) to assemble the membrane electrode. The fuel cell test was carried out at a temperature of 60 ℃ and a relative humidity of 100 % with 1.0 bar back pressures of H_2 and O_2. Additionally, the flow rates of H_2 and O_2 gases were maintained at 300 mL min^{-1} during the test.

5. Computational Details

The computational analyses presented herein were conducted using the Vienna Ab initio Simulation Package (VASP), anchored in density-functional theory (DFT). Employing the generalized gradient approximation (GGA) with the Perdew-Burke-Ernzerhof (PBE) functional addressed the exchange-correlation energy component,

while a plane-wave basis set with an energy cutoff of 400 eV was utilized. For the Brillouin-zone integrations in the supercell models, a 3×3×1 Monkhorst-Pack k-point grid was employed. The atomic positions were optimized until the forces on each atom were reduced to below 0.01eV/Å.

To evaluate the hydrogen evolution reaction (HER) catalytic activity, the free energy of hydrogen adsorption (ΔG_{H^*}) was determined using the following equation:

$$\Delta G_{H^*} = \Delta E_{H^*} + \Delta E_{ZPE} - T\Delta S_H$$

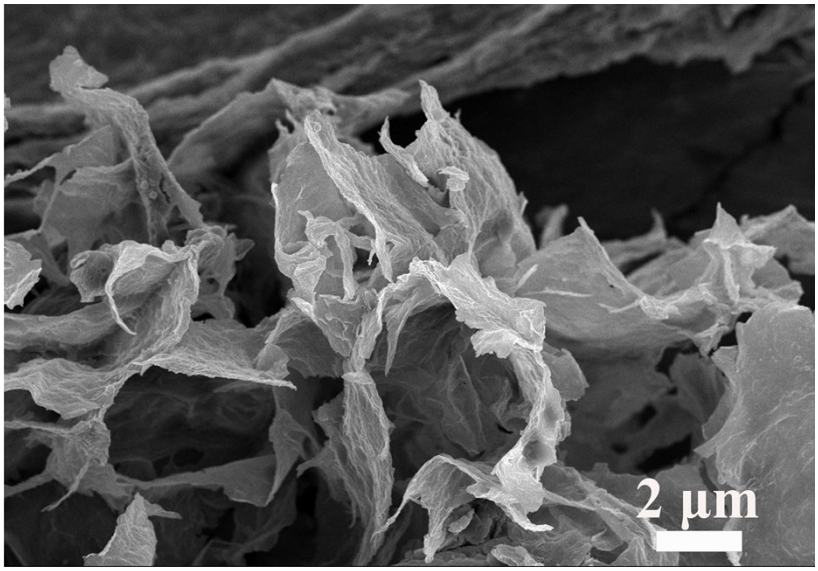

Fig. S1 SEM image of Ni/rGO.

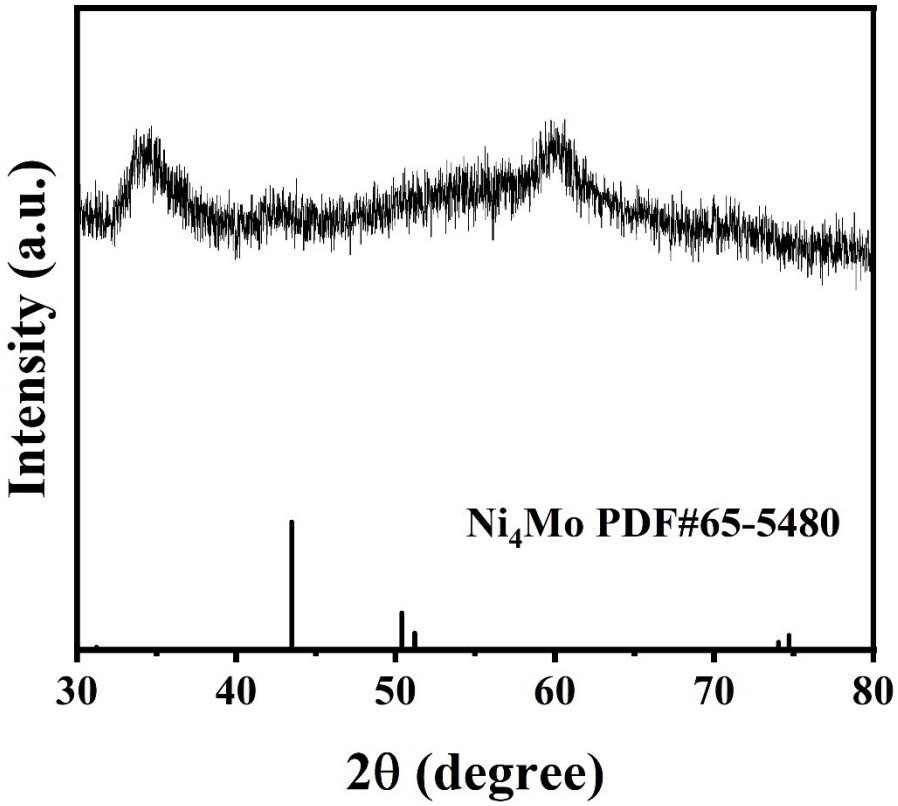

Fig. S2 XRD pattern of the precursor before heating treatment.

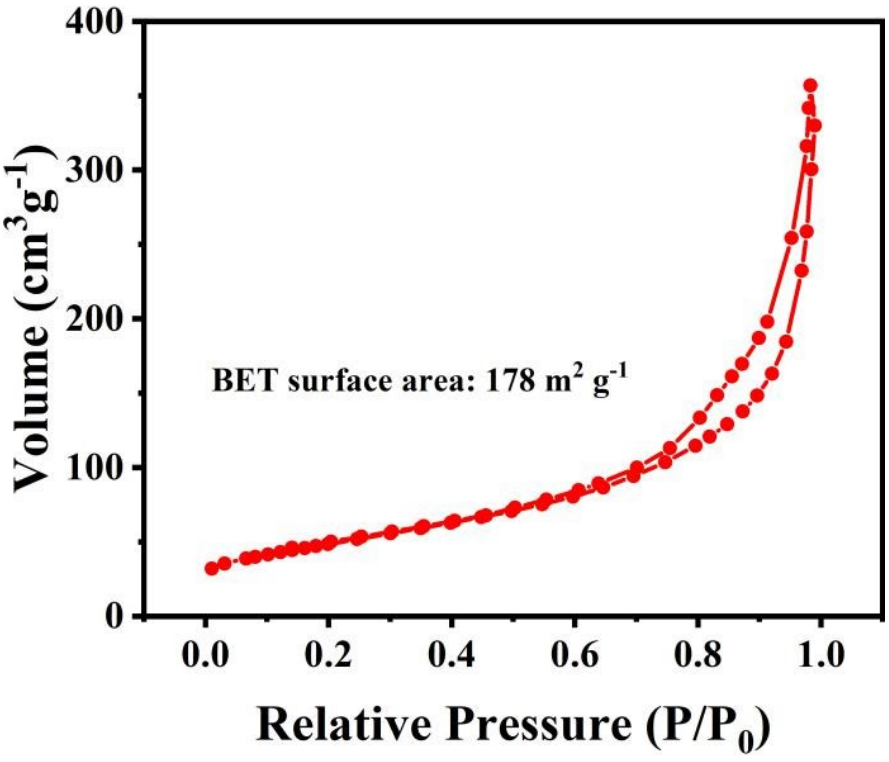

Fig. S3 N_2 adsorption-desorption isotherm of Ni_4Mo/rGO.

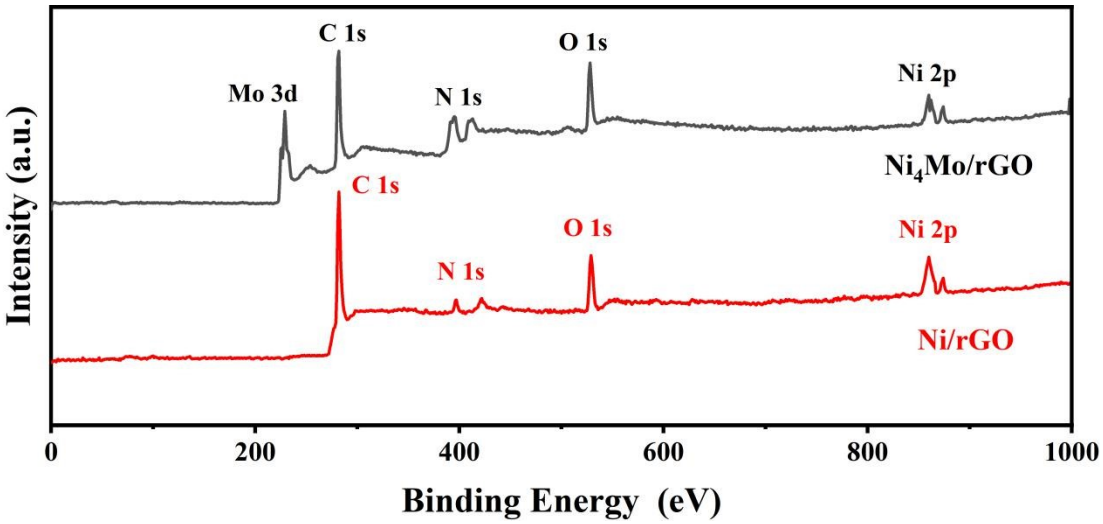

Fig. S4 Wide XPS spectra of Ni_4Mo/rGO and Ni/rGO.

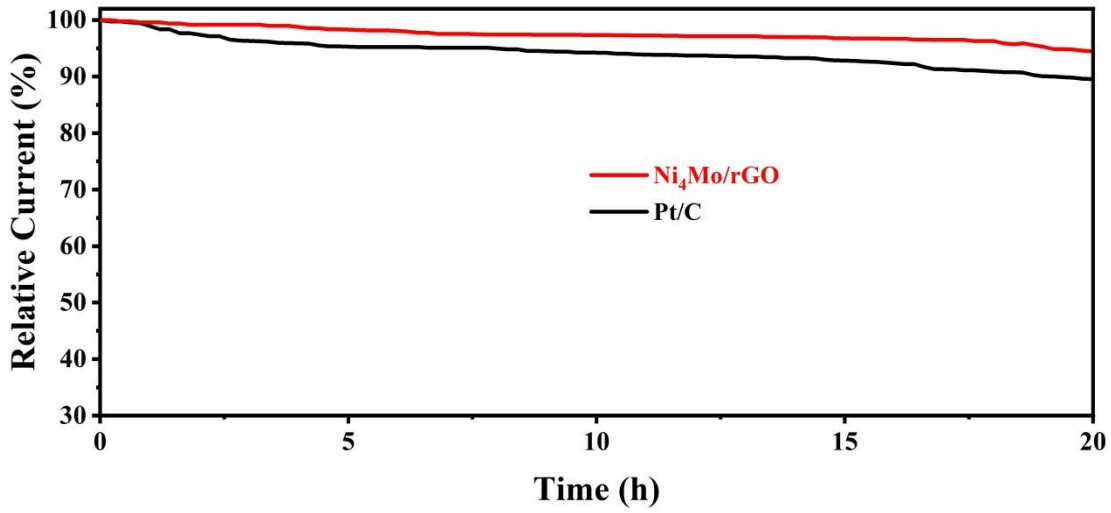

Fig. S5 Chronoamperometry response at 0.1 V (vs. RHE) of Ni_4Mo/rGO and Pt/C tested in H_2-saturated 0.1 M KOH electrolyte.

Table S1. Comparison the HOR performance of Ni_4Mo/rGO under 100mV overpotential in 0.1 M KOH with the recently reported Ni-based catalysts.

Catalysts	Loading (mg cm^{-2})	J_0 (mA cm^{-2})	References
Ni_4Mo/rGO	**0.1**	**1.63**	**This work**
np-Ni_3N	0.16	~1.7	*Energy Environ. Sci.*, 2019, 12, 3522.
NiMo/KB	0.5	~1.1	*J. Mater. Chem. A,* 2017,5, 24433.
Ni_3@(hBN)1/C - 700NH_3	0.25	~1.45	*Chem. Sci.*, 2017, 8, 5728.
Ni_4Mo/TiO_2	0.538	~2.2	*Nat. Commun.*, 2024,15, 76.
Ni_2W/TiO_2	0.751	~1.9	

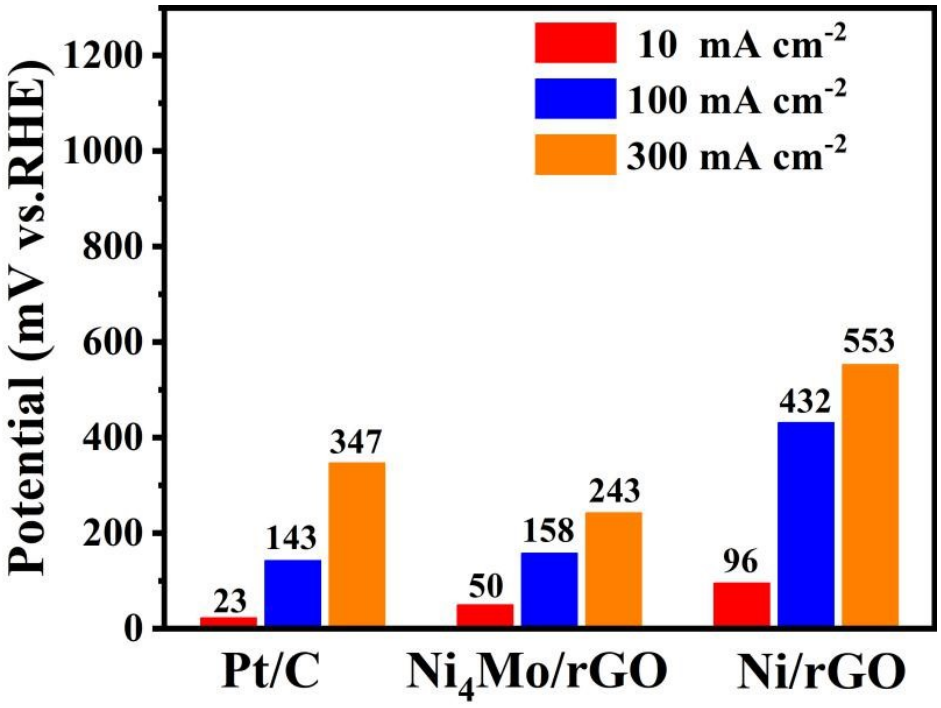

Fig. S6 HER overpotentials of Ni_4Mo/rGO, Ni/rGO and Pt/C at different current densities.

Table S2. Comparison of the HER performance of Ni_4Mo/rGO with the reported non-precious-metal-based electrocatalysts in alkaline electrolyte.

Catalysts	Overpotentials (mV@10mA cm^{-2})	References
Ni_4Mo/rGO	**51**	**this work**
SA-Mo-NC	132	*Angew. Chem. Int. Ed.*, 2017, 56, 16068.
NiMo-EDA	72	*ACS Appl. Mater. Interfaces*, 2018, 10, 1728.
NiMo-HS	38	*ACS Appl. Mater. Interfaces*, 2019, 11, 21998.
NiS_2/MoS_2 HNW	204	*ACS Catal.*, 2017, 7, 6179.
NiMo HM	72	*Appl. Catal. B-Environ.*, 2019, 249, 98.
MoxC-Ni@NCV	126	*J. Am. Chem. Soc.*, 2015, 137, 15753.

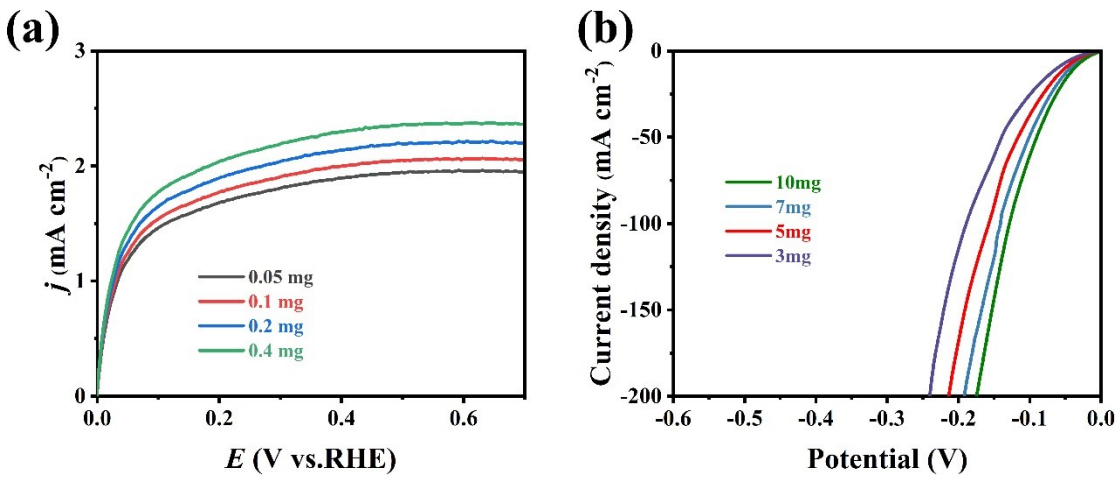

Fig. S7 (a) HOR and (b) HER polarization curves of Ni_4Mo/rGO with different loadings on electrodes.

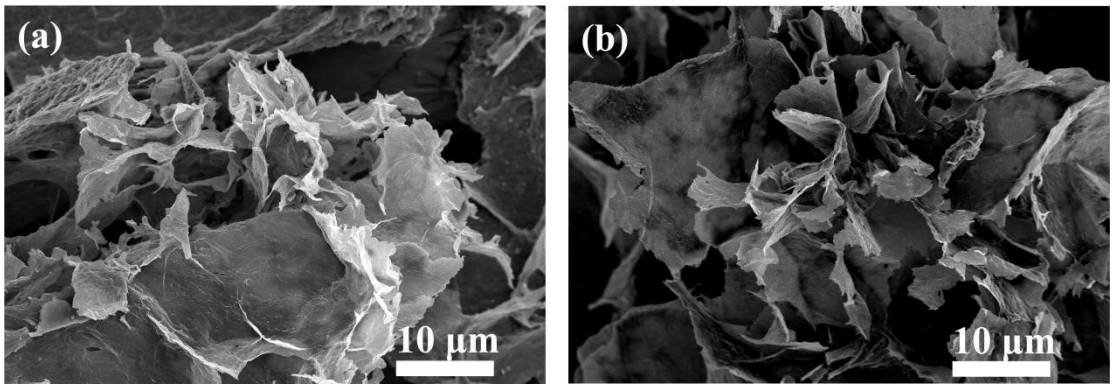

Fig. S8 SEM images of the samples prepared from different pyrolytic temperatures: (a) 400℃ and (b) 600 ℃.

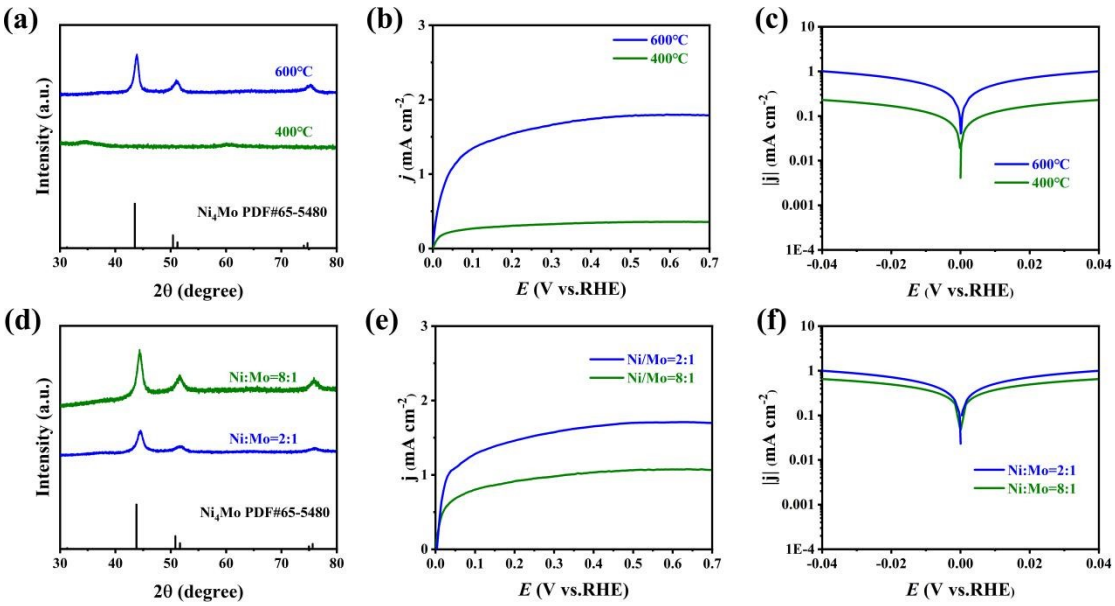

Fig. S9 (a) XRD patterns, (b) HOR polarization curves and (c)Tafel plots of the samples prepared from different pyrolytic temperatures. (d) XRD patterns, (e) HOR polarization curves and (f) Tafel plots of the samples prepared from different Ni^{2+}/ MoO_4^{2-} ions molar ratios. The electrolyte is H_2-saturated 0.1 M KOH electrolyte.

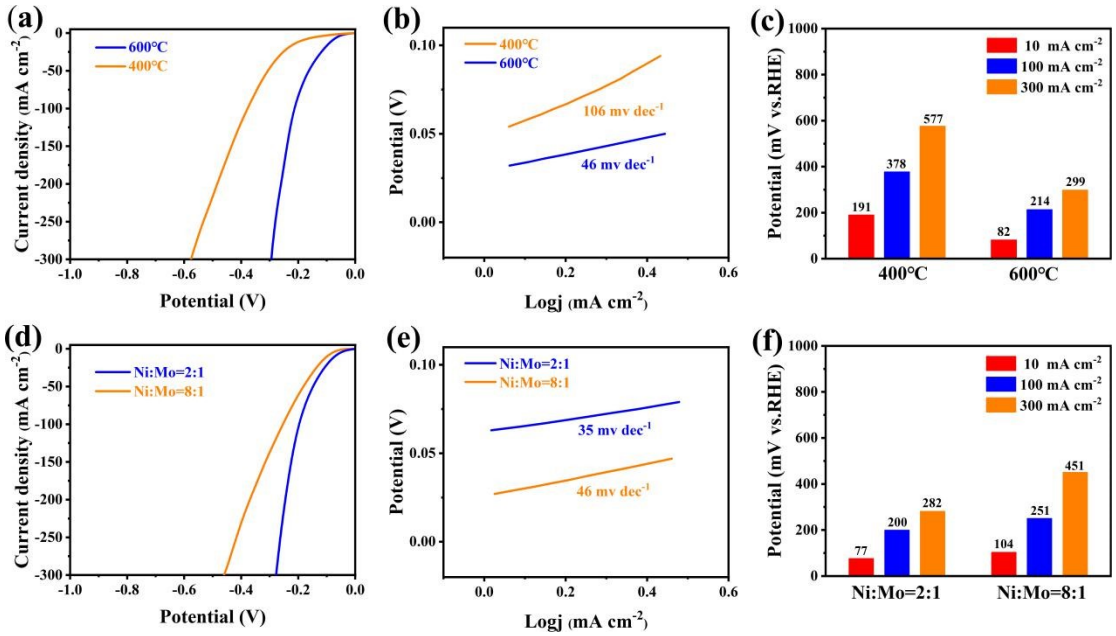

Fig. S10 (a) HER polarization curves, (b) corresponding Tafel plots and (c) overpotentials of the samples prepared from different pyrolytic temperatures tested in 1.0 M KOH electrolyte. (d) HER polarization curves, (e) corresponding Tafel plots and (f) overpotentials of of the samples prepared from different Ni^{2+}/ MoO_4^{2-} ions molar ratios tested in 1.0 M KOH electrolyte.

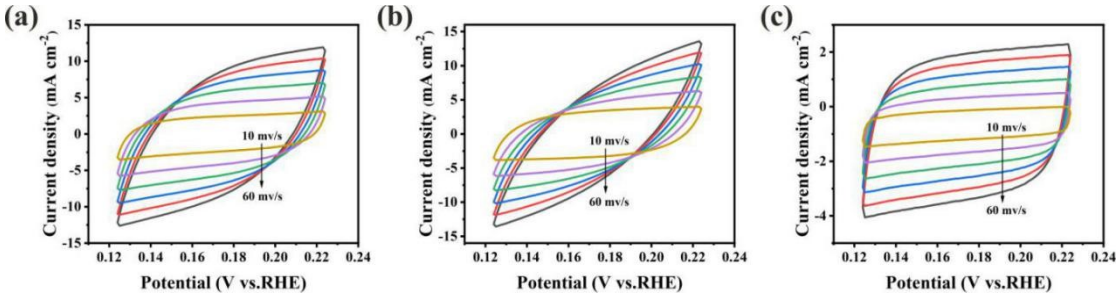

Fig. S11 CVs of (a) Ni_4Mo/rGO, (b) Ni/rGO and (c) rGO recorded at the potential of 0.12~0.22 V under different rates from 10 to 60 mV s^{-1} tested in 1.0 M KOH.

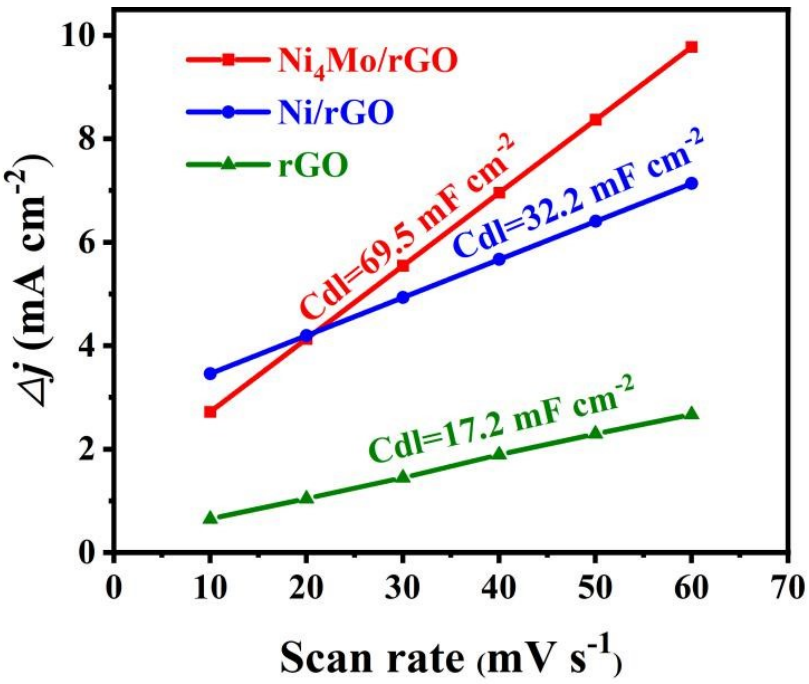

Fig. S12 The corresponding C_{dl} values derived from Fig. 12.

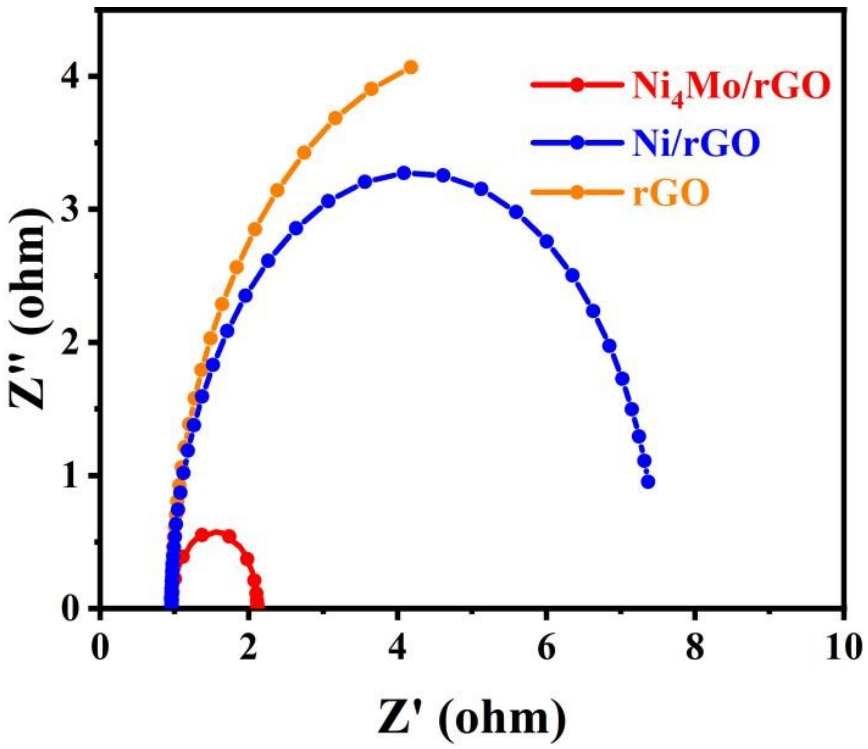

Fig. S13 Corresponding nyquist plots of Ni_4Mo/rGO, Ni/rGO and rGO tested in 1.0 M KOH electrolyte.

Table S3. Comparison the AEMFC performances of Ni-based anodic electrocatalysts.

Anode catalyst	Peak power density ($mW\ cm^{-2}$)	References
Ni_4Mo/rGO 1.5 $mg_{cat}\ cm^{-2}$	**369**	**This work**
Ni_4Mo/TiO_2 1.35$mg_{Ni}\ cm^{-2}$	520	*Nat. Commun.*, 2024, 15, 76.
Ni_4Mo 1.35 $mg_{Ni}\ cm^{-2}$	188	
Ni@Oi-Ni 1.3 $mg_{Ni}\ cm^{-2}$	200	*J. Am. Chem. Soc.*, 2022, 144, 12661.
NiMo/KB 4.0 $mg_{cat}\ cm^{-2}$	120	*Sustain. Energy Fuels*, 2018, 2, 2268.
Ni/Ni_3N-C 0.5 $mg_{metal}\ cm^{-2}$	223	*Adv. Func. Mater.*, 2021, 31, 2106156.
Ni@C 5.0 $mg_{Ni}\ cm^{-2}$	160	*ACS Appl. Mater. Interfaces*, 2020, 12, 31575.

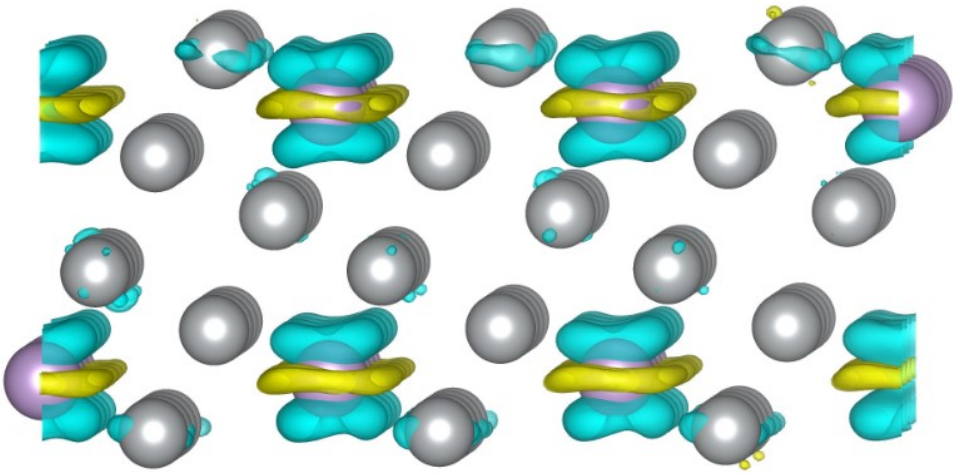

Fig. S14 The calculation model of charge density difference. Silver-white atom: Ni atoms, purple atom: Mo atoms. The blue part indicates the loss of electrons and the yellow part indicates the gain of electrons.

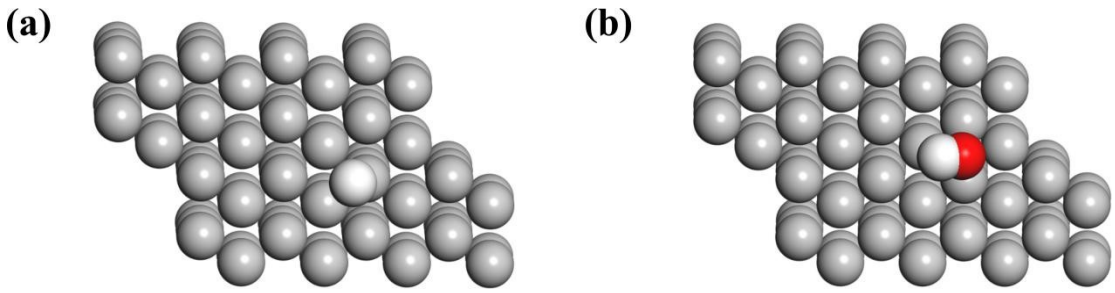

Fig. S15 Optimized structural modeling of (a) H* and (b) OH* adsorption sites on the Ni surface. The silver-white, white and red balls represent Ni, H and O atoms, respectively.

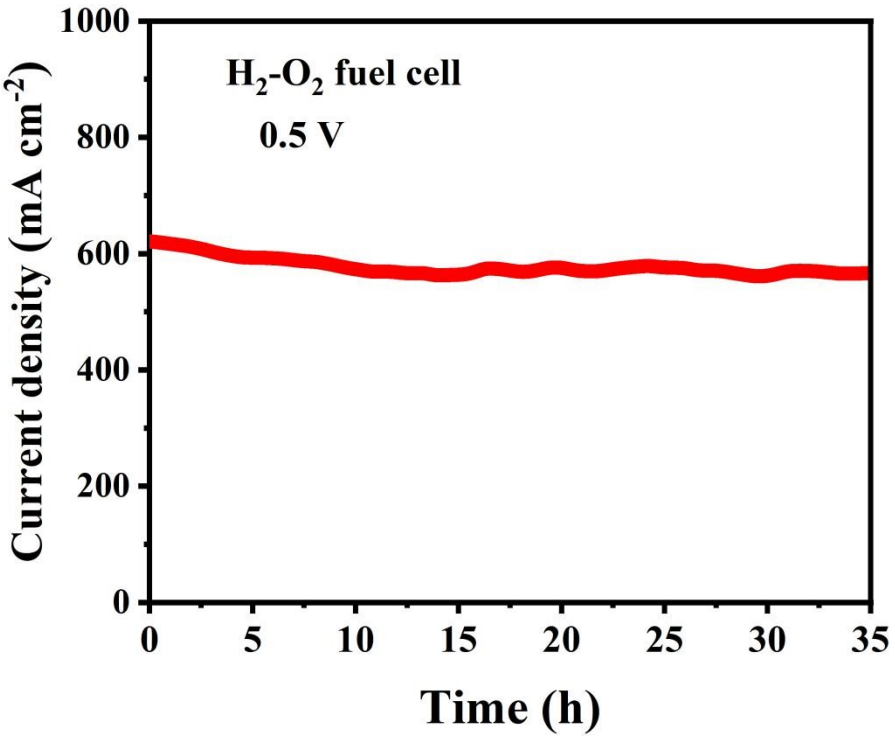

Fig. S16 Current versus time curves recorded at a constant voltage of 0.5 V based on Ni_4Mo/rGO.

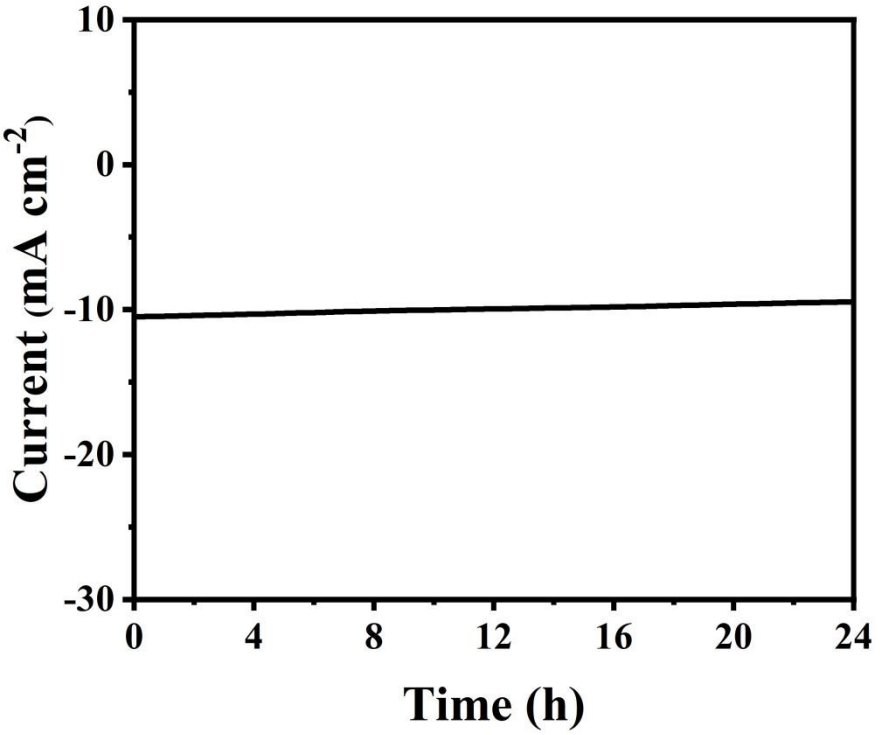

Fig. S17 I-t curve of Ni_4Mo/rGO/NF for 24h in 1 M KOH electrolyte.